Here, apart from the universal constants, ρ is the ratio of particle to TCNQ sites. The negative Seebeck coefficients observed for the dpa complexes indicate that the current carriers are electrons in the complexes. On the basis of eq 7, ρ is evaluated as 0.44–0.47 from the observed Seebeck coefficients, supporting the formula $Cu^{+}(dpa)_n(TCNQ^{0.5-})_2$.

Discussion

The above mentioned data concerning molecular arrangement in the complexes are summarized as follows: (1) the IR spectra showed the presence of single TCNQ species in every compound, (2) the magnetic susceptibility ascribed to TCNQ of each compound exhibited weak temperature dependence, which is characteristic of conducting one-dimensional solids, and (3) the ESR spectrum of $Cu(dpa)_2(TCNQ)_2$ crystals indicated that the TCNQ molecules are stacked along the needle axis. These suggest that a TCNQ column structure is formed in every $Cu(dpa)_n(TCNQ)_2$ complex as commonly found in highly conducting TCNQ salts.[1]

The results of thermoelectric power and IR experiments evidently showed that each TCNQ molecule carries a fractional charge on the average. This along with the ESR study result proposes the formula $Cu^{+}(dpa)_n(TCNQ^{0.5-})_2$. A column consisting of $TCNQ^{0.5-}$ may form a half-filled band, resulting in metal-like electric conduction. This has been demonstrated by the metal-like conductivity of $Cu(dpa)_2(TCNQ)_2$ crystals. Probably, the powder materials also have intrinsically a metallic property within powder particles (or small domains).

A broad intense band has been observed for many TCNQ salts in the near-IR region.[9,31] One of well-characterized examples is given by (tetraethylammonium)$(TCNQ)_2$,[32] which shows a broad absorption band at ca. 3000 cm^{-1} with a sharp edge at ca. 1600 cm^{-1}. This absorption band has been interpreted in terms of an electronic transition between TCNQ bands.[32] The broad intense band observed with an absorption maximum at 2900 cm^{-1} for each $Cu(dpa)_n(TCNQ)_2$ compound also can be ascribed to an electronic transition. Every spectrum displays the same absorption pattern. This may suggest that essentially the same TCNQ band structure is formed in all complexes investigated.

The copper atoms of each $Cu(dpa)_n(TCNQ)_2$ compound are practically in the +1 oxidation state. In the course of the complex formation, $Cu^{2+}(dpa)_n$ chelates oxidize $TCNQ^{-}\cdot$ partially to yield $Cu^{+}(dpa)_n(TCNQ^{0.5-})_2$. The resulting fractional charge on TCNQ leads to the metal-like conductivity in the TCNQ lattices. The copper chelates are indispensable for forming current carriers on the TCNQ arrays. An intermediate oxidation state (or mixed-valence state) of constituent molecules is one of important features found commonly in molecular metals.[1] The formation of chemical species with a mixed-valence state may be accomplished by selecting an appropriate oxidant or reductant.[33] Copper(II) chelates can function as excellent oxidizing agents against $TCNQ^{-}\cdot$ so that they can afford highly conducting TCNQ salts.

Acknowledgment. This research was supported by Grants 83-01-156-9 and 84-01-169-9 from the Secretaría de Educación Pública, Mexico. Our grateful thanks are due to Professor Q. Fernando at the University of Arizona for providing the facility to use the E-3 ESR spectrometer.

Registry No. $Cu(dpa)_2(TCNQ)_2$, 93855-33-5; $Cu(dpa)_2(TCNQ)_2\cdot H_2O$, 98194-40-2; $Cu(dpa)(TCNQ)_2$, 98194-42-4; $Cu(dpa)_2(NO_3)_2$, 14128-83-7.

Supplementary Material Available: Figures of χ vs. T plots for $Cu(dpa)_n(TCNQ)_2$ and the IR spectrum of $Cu(dpa)_2(TCNQ)_2$ (2 pages). Ordering information is given on any current masthead page.

(31) Kondow, T.; Sakata, T. *Phys. Status Solidi A* **1971**, *6*, 551. Bandrauk, A. D.; Truong, K. D.; Carlone, C.; Jandl, S.; Ishii, K. *J. Phys. Chem.* **1985**, *89*, 434.
(32) Rice, M. J.; Pietronero, L.; Bruesch, P. *Solid State Commun.* **1977**, *21*, 757.
(33) Torrance, J. B. *Acc. Chem. Res.* **1979**, *12*, 79.

Contribution from the Department of Chemistry, The Pennsylvania State University, University Park, Pennsylvania 16802

Tris(*o*-phenylenedioxy)cyclotriphosphazene: The Clathration-Induced Monoclinic to Hexagonal Solid-State Transition

Harry R. Allcock,* Michael L. Levin, and Robert R. Whittle

Received December 14, 1984

Tris(*o*-phenylenedioxy)cyclotriphosphazene (I) is known to clathrate a variety of small molecules. The clathration process coincides with a solid-state transformation of the host from a monoclinic, guest-free form to a hexagonal, guest-containing modification, a process that involves a 23% volume expansion. The transition occurs in response to improved opportunities for van der Waals attraction as guest molecules enter the lattice. Scanning electron microscopy revealed that considerable crystal disruption occurs during the transition. The resultant microcrystallites were fairly uniform in size and morphology. Crystals of I are monoclinic, space group $P2_1/n$, with eight formula units in a unit cell of dimensions a = 25.086 (5) Å, b = 5.911 (2) Å, c = 25.913 (7) Å, and β = 95.97 (2)°. The water adduct of I (II), crystallizes in the hexagonal space group $P6_3/m$ with two molecules in a unit cell of dimensions a = 11.606 (4) and c = 10.087 (3) Å. Both structures were solved by direct methods and refined by full-matrix least-squares calculations to R = 0.075 and R_w = 0.082 for 2341 reflections for I and to R = 0.050 and R_w = 0.056 for 287 reflections for II.

Introduction

Tris(*o*-phenylenedioxy)cyclotriphosphazene (I) is the simplest member of a class of spirocyclic phosphazene molecules that form tunnel inclusion adducts.[1-9] The clathration process can be used to separate different guest molecules from mixtures,[1,3] and the clathrates themselves provide a means for the storage of unstable

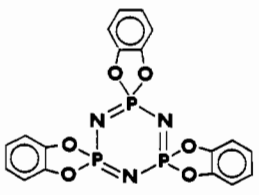

I

(1) Allcock, H. R.; Siegel, L. A. *J. Am. Chem. Soc.* **1964**, *86*, 5140.
(2) Siegel, L. A.; van den Hende, J. H. *J. Chem. Soc. A* **1967**, 817.
(3) Allcock, H. R. *Acc. Chem. Res.* **1978**, *11*, 81.
(4) Allcock, H. R.; Kugel, R. L. *Inorg. Chem.* **1966**, *5*, 1016.
(5) Allcock, H. R.; Teeter-Stein, M. *J. Am. Chem. Soc.* **1974**, *96*, 49.
(6) Allcock, H. R.; Teeter-Stein, M.; Bissell, E. C. *J. Am. Chem. Soc.* **1974**, *96*, 4795.
(7) Allcock, H. R.; Allen, R. W.; Bissell, E. C.; Smeltz, L. A.; Teeter, M. *J. Am. Chem. Soc.* **1976**, *98*, 5120.
(8) Allcock, H. R.; Ferrar, W. T.; Levin, M. L. *Macromolecules* **1982**, *15*, 697.
(9) Allcock, H. R. In "Inclusion Compounds"; Atwood, J. L., Davies, J. E. D., MacNicol, D. D., Eds.; Academic Press: New York, 1984.

0020-1669/86/1325-0041$01.50/0

molecules,[10] allow X-ray structural information to be obtained about uncrystallizable guest molecules,[8] and provide a template for the stereoregular γ-ray-induced polymerization of unsaturated guest species.[8,11]

Compound I is known to exist in two crystallographic forms. In earlier work[1] it was found from X-ray powder diffraction data that guest-free crystals of I were monoclinic or triclinic. The guest-containing forms have a hexagonal crystal structure.[1,7] The monoclinic form can be converted spontaneously to the hexagonal form by exposure of the crystals to the vapor or liquid of the guest species at room temperature. Thus, the crystal transformation accompanies the imbibition of the guest. The same crystallographic conversion can also be induced by heating the guest-free material to 170 °C.[1]

The powder diffraction results were compatible with the view that the guest-containing forms of I always have the same general lattice structure regardless of the type of guest molecules present, although the lattice expands or contracts slightly to accommodate guest molecules of different size. Moreover, the same type of adduct is formed irrespective of whether the inclusion species is prepared by recrystallization or by direct liquid or vapor imbibition. Guest molecules can be removed from I by heating the adduct under dynamic vacuum,[3] a process that results in a reversion to the monoclinic-type lattice structure.

The work carried out previously has involved single-crystal X-ray crystallography of clathrates formed between I and different organic guests,[1-8] studies of the relative ease of clathration of different guest molecules,[1] NMR studies of guest molecular motion inside the tunnel system of I,[5,12] and the behavior of clathrated unsaturated organic molecules under γ-irradiation.[8,11,13] However, no studies have been made of the crystallographic transformation itself, mainly because the crystal structure of the guest-free form was not known.

We have now investigated the crystal structure of guest-free I with a view to understanding the mechanism and driving force for the crystal transformation of the monoclinic to the hexagonal modification. Specifically, we have carried out X-ray structural analyses on guest-free I and on a water adduct of I, henceforth referred to as II.

The following questions are of particular interest with respect to this clathration system: (1) How does the host molecular packing arrangement differ in the guest-free and guest-containing structures? (2) Does a difference exist in the molecular conformation of I in the two crystal systems? (3) What is the driving force for the clathration of guests and for the concurrent crystal transformation? (4) By what intermolecular reorientation mechanism does one crystallographic form become converted to the other? (5) How do guest molecules penetrate the lattice in order to trigger the crystal transformation? (6) How long are the tunnels? Are they continuous throughout a crystallite? (7) What influence, if any, does the internal crystal structure change have on the external morphology and crystallite size?

Experimental Section

Materials. Hexachlorocyclotriphosphazene (Ethyl Corp. or Inabata) was purified by recrystallization from hexane and sublimation at 50 °C (0.1 torr). Catechol (Aldrich) was recrystallized from toluene. Anhydrous sodium carbonate (Fisher) was dried at 80 °C (0.5 torr) before use. Tetrahydrofuran (Fisher) was dried and distilled from sodium benzophenone ketyl. Xylene (Fisher) and 4-bromostyrene (Aldrich) were used as received. Acrylonitrile (Aldrich) was dried over 4-Å molecular sieves and vacuum-distilled.

Synthesis of Tris(*o*-phenylenedioxy)cyclotriphosphazene (I). Compound I was prepared by the reaction of hexachlorocyclotriphosphazene with catechol in the presence of sodium carbonate by the method described previously.[14] The product was purified by recrystallization from hot xylene followed by triple sublimation at 175 °C (0.1 torr) to give a material with a melting point at 244–245 °C.

Table I. Summary of Crystal Data and Intensity Collection Parameters

	guest-free I	H_2O-containing II
formula	$C_{18}H_{12}N_3O_6P_3$	$C_{18}H_{12}N_3O_6P_3 \cdot 2H_2O$
fw	459.23	495.27
cryst dimens, mm	0.15 × 0.17 × 0.24	0.17 × 0.18 × 0.47
method of cryst growth	sublimation	crystn from wet 4-bromostyrene
space group	$P2_1/n$	$P6_3/m$
a, Å	25.086 (5)	11.606 (4)
b, Å	5.911 (2)	
c, Å	25.913 (7)	10.087 (3)
β, deg	95.97 (2)	
vol, Å^3	3822 (3)	1177 (1)
Z	8	2
d(calcd), g/cm^3	1.596	1.398
2θ limits, deg	3.0–48.0	3.0–42.0
scan speed, deg/min	1.0–5.0	1.0–4.0
bkgd	0.5	0.5
anisotropic decay cor	0.954–1.057	0.981–1.050
no. of unique obsd data ($I > 2\sigma(I)$)	2341	287
mean discrepancy of multiply measd reflcns		0.039
μ, cm^{-1}	3.61	2.92
data/parameter	6.48	4.86
R; R_w ($=[\sum w\Delta^2/\sum wF_o^2]^{1/2}$)	0.075; 0.082	0.050 ; 0.056
goodness of fit	4.936	1.557
largest residual peak, e/Å^3	0.45	0.28
max shift/error	0.01	0.02

X-ray Structure Determinations. Our general X-ray data collection and structure refinement technique has been described previously.[15] Only details relevant to this work will be presented here. Rectangular crystals of guest-free I were grown by vacuum sublimation. Several suitable crystals were sealed within 0.2 mm wide capillaries to prevent exposure to potential guest molecules. All manipulations were made within a drybox. Crystals of II were grown by recrystallization of I from wet 4-bromostyrene. The crystals were hexagonal columns and were sealed in capillaries 0.2 mm wide to prevent loss of guest during data collection. Pertinent crystal data and the details of the structure determinations are summarized in Table I.

Of the 4690 total reflections obtained for I, 2341 were considered observed ($I > 2\sigma(I)$). For II, 2013 reflections were collected, of which 592 were unique and 287 were considered observed ($I > 2\sigma(I)$). Intensity data were corrected for Lorentz–polarization factors and anisotropic decay; the linear absorption coefficients were sufficiently small that absorption corrections were deemed unnecessary.

The structures were solved by direct methods. For I, several cycles of least-squares refinement and difference Fourier syntheses located all non-hydrogen atoms. In the final cycles of full-matrix least-squares refinement, the phosphorus, oxygen, and nitrogen atom positional parameters and anisotropic thermal parameters were refined. The carbon atom positional parameters were refined isotropically. The hydrogen atoms were fixed at calculated positions (C–H = 0.97 Å) and were given fixed, arbitrary, isotropic thermal parameters (B = 5.0 Å^2). For II, least-squares refinement and difference Fourier syntheses located all atoms except for one of the water hydrogen atoms, which has an extremely low occupancy at each of its symmetry-related positions. The positional parameters and anisotropic thermal parameters were refined for all non-hydrogen atoms of the host molecule. The oxygen atoms of the two water molecules (partial occupancy O(2) of 0.667) were refined isotropically. The hydrogen atom positional parameters were refined with isotropic thermal parameters fixed at B = 4.0 Å^2. The weights used in the refinement were derived from counting statistics. Scattering factors for H atoms were taken from those of Stewart et al,[16] and for the non-hydrogen atoms the tables of Cromer and Mann[17] were used.

Final fractional coordinates for guest-free I and the water adduct II are given in Tables II and III, respectively. Thermal parameters, root-

(10) Allcock, H. R.; Levin, M. L., unpublished results.
(11) Allcock, H. R.; Levin, M. L. *Macromolecules* **1985**, *18*, 1324.
(12) Meirovitch, E.; Belsky, I.; Vega, S. *J. Phys. Chem.* **1984**, *88*, 1522.
(13) Fintner, J.; Wegner, G. *Makromol. Chem.* **1979**, *180*, 1093.
(14) Allcock, H. R.; Walsh, E. J. *Inorg. Chem.* **1971**, *10*, 1643.
(15) Allcock, H. R.; Suszko, P. R.; Wagner, L. J.; Whittle, R. R.; Boso, B. *J. Am. Chem. Soc.* **1984**, *106*, 4966.
(16) Stewart, R. F.; Davidson, E. R.; Simpson, W. T. *J. Chem. Phys.* **1965**, *42*, 3175.
(17) Cromer, D. T.; Mann, J. B. *Acta Crystallogr., Sect. A: Cryst. Phys., Diffr., Theor. Gen. Crystallogr.* **1968**, *A24*, 321.

Table II. Fractional Atomic Positional Parameters for Guest-Free I

	x	*y*	*z*		*x*	*y*	*z*
			Molecule A				
P(1)	0.5739 (2)	0.970 (1)	0.6356 (2)	C(4)	0.5316 (8)	1.390 (4)	0.7810 (8)
P(2)	0.5886 (2)	0.817 (1)	0.5380 (2)	C(5)	0.5032 (8)	1.194 (4)	0.7883 (8)
P(3)	0.6644 (2)	0.724 (1)	0.6191 (2)	C(6)	0.5001 (7)	1.009 (4)	0.7543 (7)
N(1)	0.5534 (6)	0.940 (3)	0.5768 (5)	C(11)	0.5620 (7)	0.641 (3)	0.4537 (6)
N(2)	0.6437 (6)	0.724 (3)	0.5619 (5)	C(12)	0.5847 (7)	0.845 (3)	0.4443 (7)
N(3)	0.6278 (5)	0.850 (3)	0.6562 (5)	C(13)	0.5989 (7)	0.903 (3)	0.3965 (6)
O(1)	0.5280 (4)	0.883 (2)	0.6700 (4)	C(14)	0.5849 (7)	0.739 (3)	0.3582 (7)
O(2)	0.5742 (5)	1.232 (2)	0.6533 (4)	C(15)	0.5616 (7)	0.542 (3)	0.3673 (7)
O(11)	0.5541 (5)	0.624 (2)	0.5069 (4)	C(16)	0.5481 (7)	0.489 (3)	0.4159 (7)
O(12)	0.5961 (5)	0.975 (2)	0.4887 (4)	C(21)	0.7561 (6)	0.662 (3)	0.6565 (6)
O(21)	0.7250 (4)	0.816 (2)	0.6274 (4)	C(22)	0.7302 (7)	0.468 (3)	0.6656 (6)
O(22)	0.6777 (4)	0.478 (2)	0.6416 (5)	C(23)	0.7517 (8)	0.294 (4)	0.6954 (7)
C(1)	0.5267 (7)	1.040 (3)	0.7103 (7)	C(24)	0.8030 (8)	0.326 (4)	0.7155 (8)
C(2)	0.5515 (7)	1.241 (3)	0.7001 (6)	C(25)	0.8292 (8)	0.516 (4)	0.7078 (7)
C(3)	0.5569 (7)	1.418 (3)	0.7354 (7)	C(26)	0.8084 (8)	0.693 (4)	0.6787 (7)
			Molecule B				
P(1)	0.8660 (2)	1.012 (1)	0.4244 (2)	C(4)	0.7075 (8)	1.281 (4)	0.4864 (8)
P(2)	0.8821 (2)	0.766 (1)	0.3373 (2)	C(5)	0.7190 (9)	1.464 (4)	0.4579 (8)
P(3)	0.9651 (2)	0.840 (1)	0.4129 (2)	C(6)	0.7674 (8)	1.476 (4)	0.4351 (8)
N(1)	0.8435 (5)	0.897 (3)	0.3712 (5)	C(11)	0.8336 (7)	0.519 (3)	0.2711 (6)
N(2)	0.9422 (5)	0.749 (3)	0.3591 (5)	C(12)	0.8464 (7)	0.716 (3)	0.2471 (6)
N(3)	0.9266 (6)	0.981 (3)	0.4460 (5)	C(13)	0.8258 (7)	0.757 (3)	0.1962 (6)
O(1)	0.8502 (5)	1.275 (2)	0.4228 (4)	C(14)	0.7953 (7)	0.579 (3)	0.1705 (7)
O(2)	0.8283 (5)	0.937 (2)	0.4686 (4)	C(15)	0.7835 (7)	0.386 (3)	0.1961 (7)
O(11)	0.8569 (5)	0.517 (2)	0.3230 (4)	C(16)	0.8036 (7)	0.352 (3)	0.2487 (6)
O(12)	0.8757 (5)	0.862 (2)	0.2789 (4)	C(21)	1.0613 (7)	0.844 (3)	0.4173 (7)
O(21)	1.0180 (4)	0.987 (2)	0.4071 (4)	C(22)	1.0487 (6)	0.646 (3)	0.4409 (6)
O(22)	0.9941 (4)	0.642 (2)	0.4473 (4)	C(23)	1.0852 (7)	0.479 (3)	0.4537 (7)
C(1)	0.8001 (7)	1.294 (3)	0.4418 (7)	C(24)	1.1365 (7)	0.518 (3)	0.4433 (7)
C(2)	0.7885 (7)	1.106 (3)	0.4692 (6)	C(25)	1.1500 (8)	0.711 (4)	0.4204 (7)
C(3)	0.7402 (8)	1.093 (4)	0.4918 (7)	C(26)	1.1134 (8)	0.881 (4)	0.4070 (7)

Table III. Fractional Atomic Positional Parameters for $I \cdot H_2O$

	x	*y*	*z*
P	0.6406 (3)	0.1852 (3)	0.250
O	0.6244 (5)	0.0861 (4)	0.1309 (4)
N	0.5231 (8)	0.2138 (8)	0.250
C(1)	0.6108 (7)	−0.0299 (6)	0.1820 (6)
C(2)	0.5935 (9)	−0.1374 (8)	0.1104 (7)
C(3)	0.583 (1)	−0.2440 (8)	0.1816 (8)
H(2)	0.629 (5)	−0.104 (5)	0.028 (6)
H(3)	0.559 (5)	−0.315 (5)	0.134 (6)
		Water Molecules	
O(1)	0.000	0.000	0.000
O(2)	0.000	0.000	0.250
H(A)	0.000	0.000	−0.09 (1)
H(B)	0.000	0.000	0.15 (2)

mean-square displacements, and listings of observed and calculated structure factor amplitudes are available as supplementary material.

Scanning Electron Microscopy. An acrylonitrile adduct of I was prepared by exposure of guest-free I to liquid acrylonitrile. Excess acrylonitrile was then removed in vacuo. The polyacrylonitrile adduct was prepared by exposure of the monomer adduct to ^{60}Co γ-radiation as described previously.[11] A thin coat of gold was deposited on the samples. Scanning electron micrographs were obtained with the use of an International Scientific Instruments DS 130 electron microscope operated at an accelerating voltage of 40 kV.

Results and Discussion

Differences between the Molecular Packing Arrangements in the Two Crystalline Forms of I. Guest-free crystals of I are monoclinic. The overall packing arrangement within the unit cell is shown in Figure 1. No tunnels or cavities are evident that might accommodate guest molecules. Indeed, the molecules of I appear to make efficiency use of the available volume. Each molecule "occupies" 478 Å^3 of space in the monoclinic lattice.

By contrast, the guest-containing form (II) gives rise to a hexagonal lattice, with two phosphazene molecules and two water molecules occupying each unit cell. The water molecules occupy ~5-Å-diameter tunnels that penetrate the structure (Figure 2).

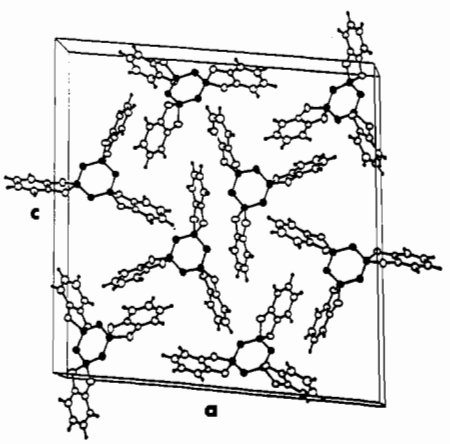

Figure 1. View of the unit cell for guest-free I. An important feature is the bending of the side groups at the oxygen atoms.

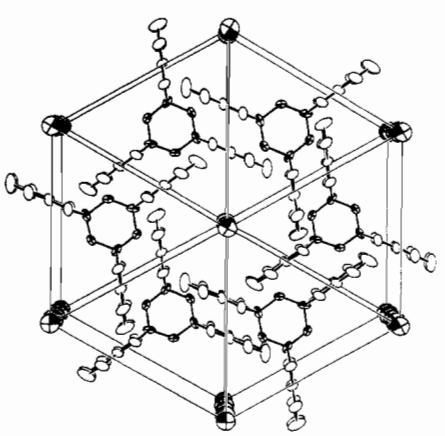

Figure 2. View down the *c* axis of three unit cells for the water adduct of I.

Table IV. Bond Lengths (Å) for Guest-Free I

	molecule A	molecule B		molecule A	molecule B
P(1)–N(1)	1.57 (1)	1.59 (1)	C(1)–C(2)	1.38 (3)	1.37 (3)
P(1)–N(3)	1.57 (2)	1.58 (1)	C(2)–C(3)	1.39 (2)	1.40 (3)
P(1)–O(1)	1.61 (1)	1.61 (1)	C(3)–C(4)	1.41 (3)	1.38 (3)
P(1)–O(2)	1.62 (1)	1.62 (1)	C(4)–C(5)	1.38 (3)	1.36 (3)
P(2)–N(1)	1.58 (2)	1.58 (2)	C(5)–C(6)	1.40 (3)	1.41 (3)
P(2)–N(2)	1.55 (2)	1.56 (1)	C(6)–C(1)	1.39 (3)	1.35 (3)
P(2)–O(11)	1.60 (1)	1.63 (1)	C(11)–C(12)	1.37 (3)	1.38 (3)
P(2)–O(12)	1.61 (1)	1.61 (1)	C(12)–C(13)	1.37 (2)	1.39 (2)
P(3)–N(2)	1.52 (1)	1.55 (1)	C(13)–C(14)	1.40 (3)	1.42 (2)
P(3)–N(3)	1.59 (2)	1.59 (2)	C(14)–C(15)	1.33 (3)	1.37 (3)
P(3)–O(21)	1.61 (1)	1.61 (1)	C(15)–C(16)	1.38 (3)	1.42 (2)
P(3)–O(22)	1.59 (2)	1.60 (1)	C(16)–C(11)	1.35 (2)	1.34 (2)
O(1)–C(1)	1.40 (2)	1.40 (2)	C(21)–C(22)	1.35 (3)	1.37 (3)
O(2)–C(2)	1.39 (2)	1.41 (2)	C(22)–C(23)	1.36 (3)	1.36 (2)
O(11)–C(11)	1.42 (2)	1.41 (2)	C(23)–C(24)	1.35 (3)	1.36 (3)
O(12)–C(12)	1.39 (2)	1.36 (2)	C(24)–C(25)	1.32 (3)	1.35 (3)
O(21)–C(21)	1.37 (2)	1.38 (2)	C(25)–C(26)	1.36 (3)	1.38 (3)
O(22)–C(22)	1.40 (2)	1.40 (2)	C(26)–C(21)	1.39 (2)	1.38 (3)

Figure 3. Side group geometry in (a) the guest-free, monoclinic form of I and (b) the clathrate-type, hexagonal modification.

In terms of the host molecules, this structure is more open than that of the monoclinic structure: each molecule of I now "occupies" 589 Å^3 of volume—a 23% increase compared to the monoclinic system. This seemingly less efficient packing arrangement is, in fact, more efficient when the presence of the guest molecules and the collinear orientation of the side groups are taken into account.

The guest-containing structure consists of alternating layers of cyclophosphazene molecules separated by approximately 5 Å. The spirocyclic side groups form the walls of the linear tunnels. This is an exceedingly efficient packing arrangement. The fact that it does not occur in the absence of guest molecules at ambient temperature suggests that the van der Waals interactions between host and guest tip the balance to stabilize the hexagonal modification (see later).

Molecular Structures of I in the Two Crystal Systems. The molecular geometries of I are similar in the two crystal systems, but with significant differences. In both systems, molecule I resembles a three-bladed paddle wheel in which the spirocyclic side groups lie perpendicular to the plane of the phosphazene ring. In the hexagonal system, the side groups are exactly radial in orientation to yield a threefold symmetric structure. In the monoclinic structure, the side groups are bent at the oxygen atoms to destroy this symmetry. This is illustrated in Figure 3. The dihedral angles (averaged for the two unique molecules in the unit cell) between the planes O–P–O and O–phenyl–O were 11.4, 20.4, and 22.4°. Apparently, the molecules of I can achieve a slightly closer packing arrangement in the guest-free form if the side groups bend away from trigonal symmetry. By contrast, the hexagonal structure, with its tunnellike pores, requires a retention of the radial symmetry shown in Figure 2.

A view of the molecular structure of the two forms of I, together with the atomic numbering scheme used, is shown in Figure 4. Interatomic distances and their esd's are listed in Table IV. Bond angles and their esd's are presented in Table V.

The Guest Molecules. The two unique water molecules were located within the tunnel system of the hexagonal form of I (Figure 5). The oxygen atoms of the guest molecules were located 2.52

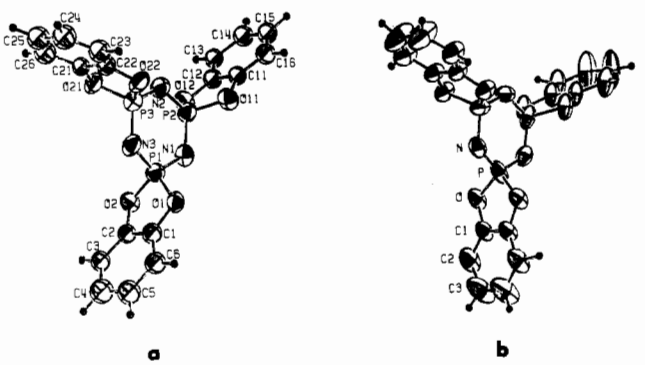

Figure 4. Molecular structures and atomic numbering schemes for (a) the guest-free form of I and (b) the water adduct of I.

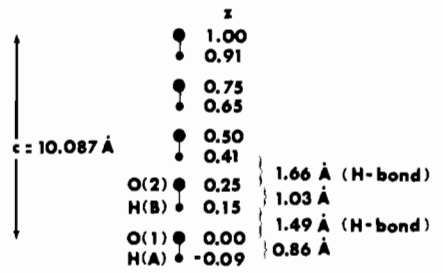

Figure 5. Schematic representation of the positions of water molecules within the tunnels of I.

Å apart along the tunnel axis (the *c* axis). Hydrogen atoms, covalently bound to each oxygen, were located also along the tunnel axis, with bonding distances of 0.86 and 1.03 Å for the two unique molecules. The hydrogen–oxygen distances *between* water molecules were 1.49 and 1.66 Å, and these values correspond to hydrogen bonds, again along the tunnel axis. The second hydrogen atom associated with each water molecule could not be located, presumably because of its random occupancy of the possible radial sites. One of the interesting features of this clathrate is that, hitherto, only organic guests have been found in the tunnel system. Clearly, small, polar, inorganic molecules can also trigger the imbibition and crystal structure transformation.

Optical and Scanning Electron Microscopy. As mentioned earlier, it was of interest to examine the effect of the crystal transformation on the external morphology of crystals of I. The monoclinic to hexagonal transition can be observed with the use of an optical microscope. For example, when a crystal of freshly sublimed I was exposed to benzene vapor in a sealed vial, the well-formed transparent crystal began to fragment within 10 s. Fractures and stress cracks appeared randomly on the surface of the crystal. Within 5 min, the crystal was deformed and completely opaque. Scanning electron micrographs were first obtained

Table V. Bond Angles (deg) for Guest-Free I

	molecule A	molecule B		molecule A	molecule B
N(1)-P(1)-N(3)	117.9 (8)	120.1 (8)	C(2)-C(1)-C(6)	122 (2)	124 (2)
N(1)-P(1)-O(1)	108.8 (7)	109.2 (7)	O(2)-C(2)-C(1)	111 (1)	112 (2)
N(1)-P(1)-O(2)	112.0 (7)	108.4 (7)	O(2)-C(2)-C(3)	126 (2)	128 (2)
N(3)-P(1)-O(1)	107.9 (7)	110.4 (8)	C(1)-C(2)-C(3)	123 (2)	120 (2)
N(3)-P(1)-O(2)	110.8 (8)	109.2 (7)	C(2)-C(3)-C(4)	116 (2)	116 (2)
O(1)-P(1)-O(2)	97.4 (6)	97.1 (6)	C(3)-C(4)-C(5)	120 (2)	123 (2)
N(1)-P(2)-N(2)	116.2 (8)	117.2 (8)	C(4)-C(5)-C(6)	124 (2)	121 (2)
N(1)-P(2)-O(11)	109.8 (7)	109.0 (8)	C(1)-C(6)-C(5)	114 (2)	117 (2)
N(1)-P(2)-O(12)	110.9 (8)	110.2 (7)	O(11)-C(11)-C(12)	110 (1)	110 (1)
N(2)-P(2)-O(11)	111.1 (8)	111.1 (8)	O(11)-C(11)-C(16)	127 (2)	124 (2)
N(2)-P(2)-O(12)	110.4 (8)	111.2 (8)	C(12)-C(11)-C(16)	123 (2)	125 (2)
O(11)-P(2)-O(12)	96.7 (6)	96.2 (6)	O(12)-C(12)-C(11)	113 (1)	114 (1)
N(2)-P(3)-N(3)	115.6 (8)	118.6 (8)	O(12)-C(12)-C(13)	124 (2)	126 (2)
N(2)-P(3)-O(21)	110.8 (8)	109.6 (7)	C(11)-C(12)-C(13)	122 (2)	120 (2)
N(2)-P(3)-O(22)	113.4 (9)	110.7 (8)	C(12)-C(13)-C(14)	113 (2)	116 (2)
N(3)-P(3)-O(21)	111.0 (7)	108.6 (8)	C(13)-C(14)-C(15)	124 (2)	121 (2)
N(3)-P(3)-O(22)	108.6 (8)	110.4 (7)	C(14)-C(15)-C(16)	121 (2)	121 (2)
O(21)-P(3)-O(22)	95.8 (7)	96.7 (6)	C(11)-C(16)-C(15)	116 (2)	116 (2)
P(1)-N(1)-P(2)	121.3 (9)	120.8 (9)	O(21)-C(21)-C(22)	114 (1)	113 (1)
P(2)-N(2)-P(3)	126 (1)	124 (1)	O(21)-C(21)-C(26)	127 (2)	127 (2)
P(1)-N(3)-P(3)	122.5 (9)	119.1 (9)	C(22)-C(21)-C(26)	119 (2)	119 (2)
P(1)-O(1)-C(1)	106 (1)	107 (1)	O(22)-C(22)-C(21)	109 (1)	110 (1)
P(1)-O(2)-C(2)	107 (1)	106 (1)	O(22)-C(22)-C(23)	126 (2)	127 (2)
P(2)-O(11)-C(11)	108 (1)	109 (1)	C(21)-C(22)-C(23)	125 (2)	123 (2)
P(2)-O(12)-C(12)	108 (1)	110 (1)	C(22)-C(23)-C(24)	114 (2)	117 (2)
P(3)-O(21)-C(21)	109 (1)	107 (1)	C(23)-C(24)-C(25)	122 (2)	121 (2)
P(3)-O(22)-C(22)	111 (1)	108 (1)	C(24)-C(25)-C(26)	124 (2)	122 (2)
O(1)-C(1)-C(2)	113 (2)	112 (2)	C(21)-C(26)-C(25)	115 (2)	117 (2)
O(1)-C(1)-C(6)	125 (2)	125 (2)			

Table VI. Bond Lengths and Angles for $I \cdot H_2O$[a]

		Bond Lengths, Å			
P-O	1.608 (4)	C(1)-C(1)^{II}	1.372 (11)	C(2)-H(2)	0.93 (5)
P-N	1.555 (8)	C(1)-C(2)	1.367 (9)	C(3)-H(3)	0.87 (6)
P-N^{I}	1.581 (8)	C(2)-C(3)	1.382 (10)	O(1)-H(A)[b]	0.86 (12)
O-C(1)	1.375 (7)	C(3)-C(3)^{II}	1.379 (14)	O(2)-H(B)[b]	1.03 (16)
		Bond Angles, deg			
O-P-O^{II}	96.7 (3)	P-N-P^{III}	122.8 (6)	C(1)-C(2)-H(2)	105 (4)
O-P-N	110.5 (3)	O-C(1)-C(1)^{II}	112.0 (3)	C(3)-C(2)-H(2)	132 (4)
O-P-N^{I}	110.0 (3)	O-C(1)-C(2)	126.1 (6)	C(2)-C(3)-C(3)^{II}	121.3 (4)
N-P-N^{I}	117.2 (6)	C(2)-C(1)-C(1)^{II}	121.9 (4)	C(2)-C(3)-H(3)	114 (4)
P-O-C(1)	109.6 (3)	C(1)-C(2)-C(3)	116.8 (6)	H(3)-C(3)-C(3)^{II}	124 (4)

[a] Symmetry operations: (I) $-y, x-y, z$; (II) $x, y, {}^1/_2 - z$; (III) $y-x, \bar{x}, z$. [b] Water molecules.

of crystals of guest-free I that had been purified by vacuum sublimation. The micrographs showed that the material was highly crystalline, with typical crystal dimensions of 50 × 50 × 150 μm or larger. The crystals were generally well formed, with featureless surfaces. Exposure of these crystals to the atmosphere resulted in fragmentation as water molecules were imbibed and as the monoclinic to hexagonal transition took place. Broad-line ^1H NMR spectroscopy has been used to confirm that water molecules can enter the tunnels.[8]

Exposure of monoclinic I to water in a liquid medium brought about a rapid disintegration of the crystals to give fairly uniform microcrystallites with typical dimensions of 1 × 1 × 5 μm. Similarly, treatment of monoclinic I with liquid acrylonitrile causes crystal disintegration. The fragmentation process may be governed by the mosaic character of the original monoclinic crystals. A typical monoclinic crystal fragments into 10^5–10^6 microcrystallites on clathration. It seems likely that the microcrystallites have continuous tunnels that penetrate the entire *c*-axis lengths of the fragments.

For example, high polymers obtained by the γ-irradiation of imbibition adducts of I with vinyl monomers typically have extended chain lengths of approximately 1 μm.[11] This suggests that the tunnels penetrate a considerable fraction and possibly the entire length of the microcrystallites. (It is highly unlikely that a single polymer chain would pass through more than one microcrystallite.) The irradiation process had little effect on the dimensions or character of the microcrystallites.

Clathrate crystals obtained by recrystallization rather than direct guest imbibition are much larger, being comparable in size to the monoclinic crystals obtained by sublimation.

Mechanism of the Monoclinic to Hexagonal Crystal Transition. The scanning electron microscopy results, in conjunction with the known chain lengths of clathrate-synthesized polymers, lead us to believe that the tunnels in the hexagonal microcrystallites penetrate several thousand layers of phosphazene molecular layers, each layer being separated by 5 Å. This continuity implies that the solid-state transition from monoclinic to hexagonal occurs over that same crystalline distance before fragmentation of the crystal occurs.

It seems unlikely that an instantaneous, synchronous switching of molecular orientations throughout the crystal occurs when guest molecules penetrate the outer lattice. The very large volume change would create serious internal stresses that would probably disrupt the crystals into fragments much smaller than those detected. Moreover, this mechanism would require that guest molecules entering the crystalline faces would stimulate a host transition throughout the crystal—including regions several thousands of angstroms distant from the sites of initial stimulus.

It is more likely that the crystal transition is a stepwise process. Guest molecules may first initiate the transition at the surface. A transition zone, perhaps containing an amorphous interface, could then propagate through the monoclinic lattice, leaving the hexagonal arrangement in its wake. The tunnels formed at the transition interface would serve as conduits for the penetration

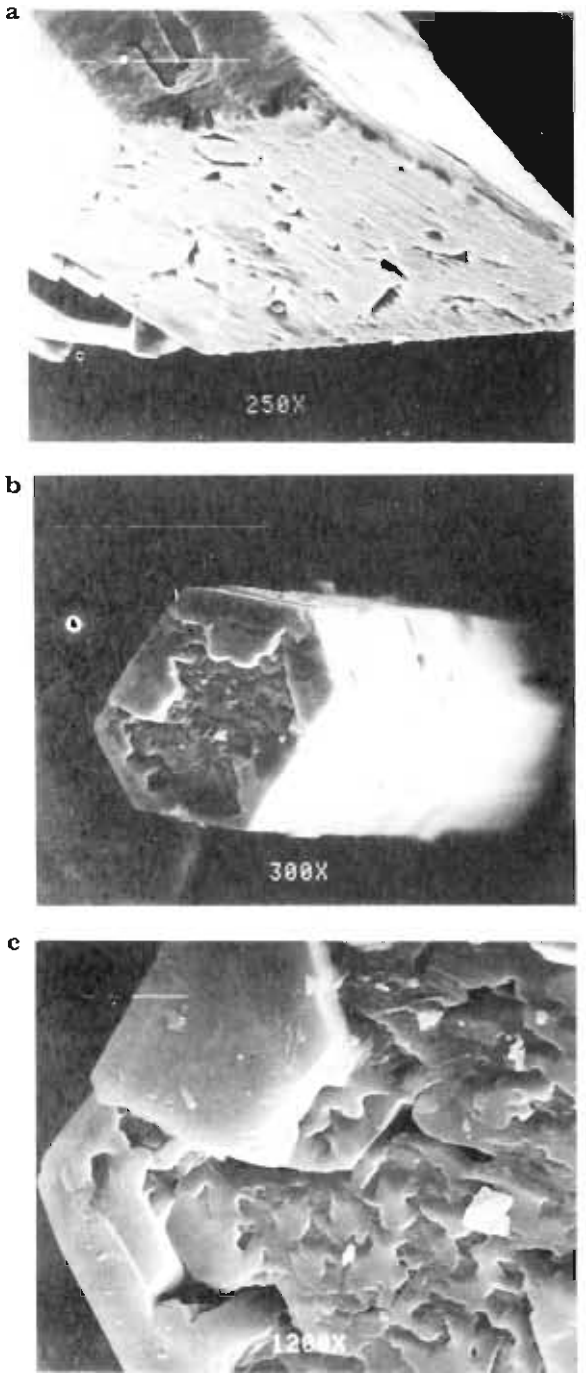

Figure 6. Scanning electron micrographs of crystals of (a) an adduct of I with benzene, (b) a similar crystal after being heated in a dynamic vacuum, and (c) a further magnification of the end face of the crystal shown in (b). For (a) and (b) the bar represents 100 μm. In (c) the bar corresponds to 10 μm.

of additional guest molecules. This would permit the transition zone to move from the surface into the interior of each crystal. Presumably crystal disruption into crystallites takes place either when the progress of the transition zone is too rapid to be accommodated by the flexibility of the crystal or when the zone reaches regions of crystal dislocations or other defect sites.

The reverse transition, i.e. hexagonal clathrate to guest-free monoclinic form, is a more difficult process to study. Very low concentrations of guest remaining in the crystals can stabilize the hexagonal structure. However, in an attempt to probe this transition, a benzene adduct of I was heated in a dynamic vacuum at 85 °C for 5 weeks. The original, well-formed crystals (prepared by recrystallization of I from benzene) fragmented but at a considerably slower rate than occurs for the monoclinic to hexagonal transition. Moreover, the transformation to the guest-free form occurs in one direction relative to the crystal morphology. Only the ends of the hexagonal rods appear to be disrupted (Figure 6). This is a consequence of the collinear nature of the tunnels. Guest molecules can presumably only be removed from one direction (along the tunnel axis). This contrasts with the monoclinic to hexagonal transition, for which no preferred entry points into the monoclinic lattice could be identified.

As guest molecules are removed, the interactions between host molecules are no longer sufficient to support the structure. The structure collapses into the less open, but now more stable, monoclinic lattice. At temperatures above 170 °C, however, the hexagonal form of I is stable in the absence of included molecules.[1] For example, when guest-free I was heated to 170 °C, the X-ray powder pattern changed and suggested that both the monoclinic and hexagonal forms were present. Moreover, guest molecules were removed when adducts of I were heated to 170 °C in the atmosphere. When crystals were cooled, they fragmented and reverted to the monoclinic lattice.[3] Thus, the monoclinic to hexagonal transition appears to be reversible.

Role of the Guest Molecules. A surprisingly wide variety of guest molecules stimulates the transition of I from monoclinic to hexagonal,[1,3,8,11] and the hexagonal framework is remarkably similar for this range of guest molecules. This insensitivity of the host lattice to the type of guest molecule is typical of several classes of tunnel clathrate systems.[18]

What is the relationship between host I and its guests? What tips the balance between the system's preference of the monoclinic or hexagonal structures?

Earlier differential thermal analysis experiments indicated that the clathration of guest molecules by I is exothermic[1] and that the loss of guest molecules is endothermic.[5] The magnitude of the change in enthalpy for both processes must be equal but opposite in sign. The energy of activation for clathration is evidently very small since the imbibition of guests occurs spontaneously at room temperature. By contrast, the opposite process—the removal of guest from the tunnels—is slow and presumably has a high energy by barrier.

All the evidence favors the view that the host–guest van der Waals attractions play a major role in stabilizing the hexagonal crystal structure. Imbibition of guest molecules offers opportunities for enhanced intermolecular interactions in spite of the required expansion of the crystal lattice. What is especially interesting is that, once formed, the hexagonal system retains its integrity even when most of the guest molecules have been removed. This could be taken as evidence that the guest molecules function as templates for the growth of the tunnel system. Although this argument might be plausible when chains of hydrogen-bonded guests, such as water molecules, are involved, it is not compatible with the shapes and character of the wide variety of organic guest molecules that induce the same crystal transition. Moreover, all attempts to induce the growth of hexagonal crystals of I around "templates" of preformed linear polymer molecules have so far proved unsuccessful.[19]

Thus, we conclude that the role of the guest is to provide enhanced opportunities for the spirocyclic side groups of I to engage in host–guest van der Waals attractions without a significant diminution in the interactions between the side groups themselves. Because other spirocyclic phosphazenes behave in the same way,[3-6,8] it seems likely that the overall phenomenon is a consequence of the molecular shape and of the nuances of shape fitting in a crystal lattice, rather than a special property of phosphazenes.

Acknowledgment. This work was supported by the National Science Foundation Polymers Program, through Grant No. DMR 81-19934 #2. We thank D. W. Strickler of the Materials Research Laboratory of this university for the electron micrographs and Dr. M. Parvez for helpful discussions. The X-ray diffraction

(18) Fetterly, L. C. In "Non-Stoichiometric Compounds"; Mandelkorn, L., Ed.; Academic Press: New York, 1964; Chapter 8.
(19) Allcock, H. R.; Smeltz, L. A., unpublished results.

data were obtained with the use of equipment purchased through a DOD instrumentation grant provided by the U.S. Army Research Office through Grant No. DAAG29-83-G0101.

Registry No. I, 311-03-5; II, 99476-97-8; hexachlorocyclotriphosphazene, 940-71-6; catechol, 120-80-9.

Supplementary Material Available: Tables of thermal parameters, root-mean-square displacements, and observed and calculated structure factor amplitudes for both structures (15 pages). Ordering information is given on any current masthead page.

Contribution from the Department of Chemistry, University of Calgary, Calgary, Alberta, Canada T2N 1N4

Preparation of Six- and Eight-Membered Mixed Cyanuric-Thiazyl Rings, $(R_2NCN)_x(NSCl)_2$ (x = 1, 2), and the X-ray Crystal Structure of $(Et_2NCN)(NSCl)_2$

T. Chivers,* J. F. Richardson, and N. R. M. Smith

Received May 21, 1985

The reaction of dialkylcyanamides with NSCl units generated from $(NSCl)_3$ in CCl_4 at ca. 60 °C produces either the six-membered rings $(R_2NCN)(NSCl)_2$ (R = Me, Et, *i*-Pr) or, in the presence of a large excess of Me_2NCN, the eight-membered ring 1,3-$(Me_2NCN)_2(NSCl)_2$. In contrast, the addition of $(C_6H_{11})_2NCN$ to a warm solution of $(NSCl)_3$ in CCl_4 yields $(C_6H_{11})_2NC(Cl)NS_3N_2^+Cl^-$, a derivative of a five-membered S_3N_2 ring, which can also be prepared by the reaction of $(C_6H_{11})_2NCN$ with $S_3N_2Cl_2$ in CH_2Cl_2 at 23 °C. Oxidative addition of Cl_2 (as SO_2Cl_2) to 1,5-$(Me_2NCN)_2(SN)_2$ gives 1,5-$(Me_2NCN)_2(NSCl)_2$. The latter is thermally more stable than the structural isomer, 1,3-$(Me_2NCN)_2(NSCl)_2$, which undergoes ring contraction, with loss of Me_2NCN, in acetonitrile at 25 °C. The mechanism of the cycloaddition reaction of R_2NCN with NSCl units is discussed. The crystal structure of $(Et_2NCN)(NSCl)_2$, determined by X-ray crystallography, shows that the exocyclic chlorine substituents adopt a cis configuration with respect to the almost planar CN_3S_2 ring. Crystal data: monoclinic, space group $P2_1/n$, a = 9.464 (3) Å, b = 8.921 (1) Å, c = 13.421 (4) Å, β = 108.29 (1)°, V = 1075.9 (5) Å^3, Z = 4. The final R and R_w values were 0.043 and 0.044, respectively.

Introduction

The preparation and X-ray structure of the six-membered mixed thiazyl-cyanuric ring **1** (R = Me_2N) via the cyclocondensation reaction between an amidine and $S_3N_2Cl_2$ was reported recently by Roesky et al., but the yield of **1** was only 7% (based on $S_3N_2Cl_2$).[1] During the course of the present study,[2] Mews et al.

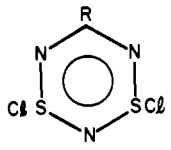

1

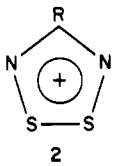

2

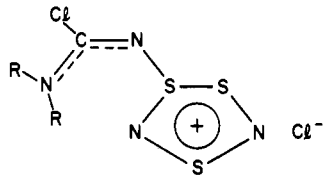

3

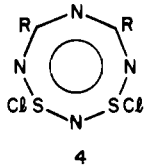

4

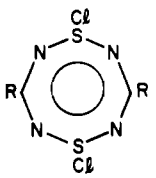

5

isolated **1** (R = CF_3) in 21% yield from the reaction of CF_3CN with $(NSCl)_3$ in an autoclave at 50 °C.[3] The five-membered ring **2**, $RCN_2S_2^+$ (R = CF_3), which is normally obtained in the reactions of organic nitriles with $(NSCl)_3$ at reflux,[4] was the major product (45%).[3]

We describe here a convenient, high-yield synthesis of **1** (R = Me_2N, Et_2N, *i*-Pr_2N) by the cycloaddition reaction of dialkylcyanamides with NSCl units generated from $(NSCl)_3$ in CCl_4 at ca. 60 °C. With $(C_6H_{11})_2NCN$, however, the same procedure gives **3** (R = C_6H_{11}), a derivative of a five-membered S_3N_2 ring, which is formally related to **2** by the addition of one NSCl unit.

In the presence of excess Me_2NCN the cycloaddition reaction produces the heterocycle **4** (R = Me_2N), the first example of an eight-membered mixed thiazyl-cyanuric ring. The structural isomer **5** is obtained by the oxidative addition of Cl_2 across the S-S bond of 1,5-$Me_2NC(NSN)_2CNMe_2$. The possible involvement of the dimeric species $(NSCl)_2$ in the cycloaddition reaction, as speculated by Mews et al.,[3] is discussed. The X-ray crystal structure of **1** (R = Et_2N) is also described.

Experimental Section

Reagents and General Procedures. Solvents were dried (carbon tetrachloride and methylene dichloride (P_2O_5), *n*-pentane (CaH_2), and acetonitrile (CaH_2 and P_2O_5)) and freshly distilled before use. All reactions and the manipulation of moisture-sensitive products were carried out under an atmosphere of dry nitrogen (99.99%). Chemical analyses were performed by the Analytical Services of the Department of Chemistry, University of Calgary, and by MHW Laboratories, Phoenix, AZ.

The following reagents were prepared by literature procedures: $(NSCl)_3$,[5] $(C_6H_{11})_2NCN$,[6] 1,5-$Me_2NC(NSN)_2CNMe_2$.[7] Other chemicals were commercial products used as received: Me_2NCN, Et_2NCN, and *i*-Pr_2NCN (Aldrich). Sulfuryl chloride (Aldrich) was distilled before use.

Instrumentation. Infrared spectra were recorded as Nujol mulls (CsI windows) on a Nicolet 5DX FT-IR spectrometer. NMR spectra were

(1) Roesky, H. W.; Schäfer, P.; Noltemeyer, M.; Sheldrick, G. M. *Z. Naturforsch., B: Anorg. Chem., Org. Chem.* **1983**, *38B*, 347.
(2) A preliminary account of this work was presented at the symposium "Horizons in the Chemistry and Properties of Low Dimensional Solids", PAC-CHEM Conference, Dec 1984, Honolulu, HI. Chivers, T.; Richardson, J. F.; Smith, N. R. M. *Mol. Cryst. Liq. Cryst.* **1985**, *125*, 447.
(3) Höfs, H.-U.; Hartmann, G.; Mews, R.; Sheldrick, G. M. *Z. Naturforsch., B: Anorg. Chem., Org. Chem.* **1984**, *39B*, 1389.
(4) Alange, G.; Banister, A. J.; Bell, B.; Millen, P. W. *J. Chem. Soc., Perkin Trans. 1* **1979**, 1192. Banister, A. J.; Smith, N. R. M.; Hey, R. G. *J. Chem. Soc., Perkin Trans. 1* **1983**, 1181.
(5) Alange, G. G.; Banister, A. J.; Bell, B. *J. Chem. Soc., Dalton Trans.* **1972**, 2399.
(6) Forman, S. E.; Erikson, C. A.; Adelman, H. *J. Org. Chem.* **1963**, *28*, 2653.
(7) Ernest, I.; Holick, W.; Rihs, G.; Schomburg, D.; Shoham, G.; Wenkert, D.; Woodward, R. B. *J. Am. Chem. Soc.* **1981**, *103*, 1540.

0020-1669/86/1325-0047$01.50/0